Available online at www.sciencedirect.com
ScienceDirect
Journal of Power Sources 166 (2007) 462–470
JOURNAL OF POWER SOURCES
www.elsevier.com/locate/jpowsour

High-energy-density hybrid electrochemical capacitor using graphitizable carbon activated with KOH for positive electrode

Taira Aida [a,*], Ichiro Murayama [a], Koji Yamada [a], Masayuki Morita [b]

[a] *Advanced Technical Development Division, Daihatsu Motor Co. Ltd., 3000 Yamanoue, Ryuo, Gamo, Shiga 520-2593, Japan*
[b] *Department of Applied Chemistry, Graduate School of Science and Engineering, Yamaguchi University, 2-16-1 Tokiwadai, Ube 755-8611, Japan*

Received 17 November 2006; received in revised form 14 January 2007; accepted 16 January 2007
Available online 26 January 2007

Abstract

A high-energy-density hybrid electrochemical capacitor (HEC) has been developed. The advanced HEC has graphitizable carbon activated with KOH (KOH-activated soft carbon) for the positive electrode instead of activated carbon, which is used in a conventional HEC or an electric double-layer capacitor (EDLC). The KOH-activated soft carbon had low electrostatic capacitance due to its small specific surface area in the initial state; however, the capacitance increased significantly by the first charging at potential over 4 V versus Li/Li$^+$ and exceeded the capacitance of activated carbon. The resulting capacitance was affected by the type of anion species and organic solvent of the electrolyte. In charge–discharge tests using various kinds of electrolytes, the KOH-activated soft carbon showed the best performance in the electrolyte of $LiPF_6$ dissolved in a binary solvent composed of ethylene carbonate (EC) and dimethyl carbonate (DMC). The advanced HEC using KOH-activated soft carbon for the positive electrode gave about 8.5 times the energy density of the conventional EDLC.

Keywords: Li-ion; Capacitor; Asymmetric capacitor; Nanogate carbon; Automotive

1. Introduction

The hybrid electric vehicle (HEV) has continued to gain popularity against the backdrop of increasing global concern for the environment and the rising cost of fossil fuels since the HEV has been commercialized in 1997. Moreover, the fuel cell electric vehicle (FCEV) is being developed actively for commercialization.

In these ecologically friendly and economical vehicles, a rechargeable battery is used to assist the peak power required and to recover the braking energy generated; this influences the performance, durability and cost of the vehicles. Nickel–metal hydride batteries (Ni–MH) have been used in commercialized HEVs, but they will be replaced with the lithium-ion battery (LIB), which has higher energy density and higher power density. An electric double-layer capacitor (EDLC) is also being examined for this application because of its excellent power density and long cycle life [1–3]. However, the energy density of an EDLC is so much lower than LIB that its usage in a vehicle is limited to only momentary power supply.

In recent years, several types of so-called hybrid electrochemical capacitors (HECs), which combine a faradically rechargeable battery-type electrode and a non-faradically rechargeable (polarizable) electrode, have been proposed [4–19]. HECs have higher energy density than EDLCs, and higher power density than pure battery systems. The HEC, which combine a disordered carbon for negative electrode with an activated carbon for positive electrode, are especially promising as a power source for HEVs and FCEVs because of the higher energy density brought by the higher capacity of the Li insertion-type anode and the higher cell voltage [4–10].

The specific capacity of the activated-carbon positive electrode in the HEC is much lower than that of the negative electrode. Therefore, the positive electrode must have a large volume—about 10 times that of the negative electrode-making the energy density of the HEC only a few times higher than that of conventional EDLCs. To achieve even higher energy density in the HEC, the capacity of the positive electrode must be improved. Extending the potential range of positive electrode to a lower potential region has been proposed to achieve this end

* Corresponding author. Tel.: +81 748 57 1685; fax: +81 748 57 1064.
E-mail address: Taira_Aida@mail.daihatsu.co.jp (T. Aida).

0378-7753/$ – see front matter © 2007 Elsevier B.V. All rights reserved.
doi:10.1016/j.jpowsour.2007.01.037

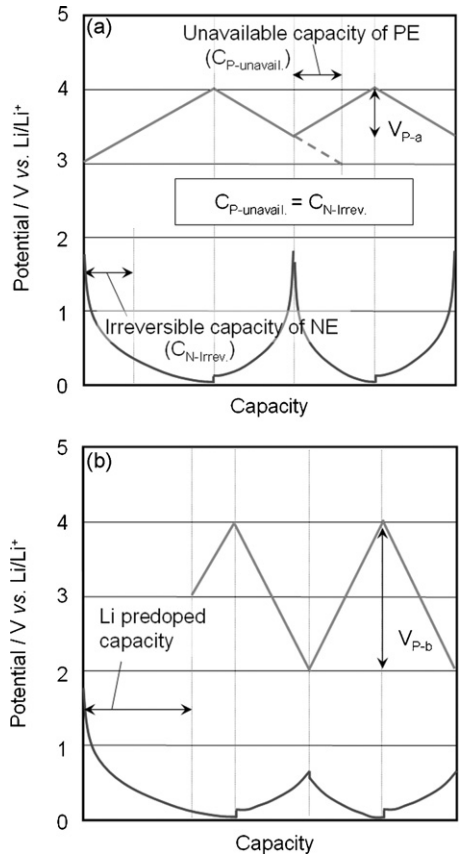

Fig. 1. Typical charge–discharge profiles of (a) conventional HEC and (b) proposed HEC, for which the potential of the positive electrode was extended to the lower potential region.

[7,8]. The typical charge–discharge profiles of the conventional HEC and proposed HEC, for which the potential of the positive electrode was extended to a lower potential region, are shown in Fig. 1. In the conventional HEC, the positive electrode can be charged and discharged at a potential range approximately 3–4 V versus Li/Li^+. However, the potential range narrows from about 3.3–4 V versus Li/Li^+ in actuality because the negative electrode has inevitable irreversible capacity, which prevents the positive electrode from discharging fully [Fig. 1(a)]. In the proposed HEC, on the other hand, the preliminary charging of the negative electrode can compensate for the irreversible capacity. Moreover, it can also improve the capacity of the positive electrode by extending the potential range to the lower potential region [Fig. 1(b)]. This method reduces the amount of material required for the positive electrode by about one third, which leads to be improved the energy density. However, a lithium auxiliary electrode must be placed in the cell and the preliminary charging of the negative electrode must be carried out during a production process.

In contrast, the capacity of the positive electrode is also improved by extending the potential range to a higher potential region. However, the upper potential limit of the positive electrode is usually controlled to below 4 V versus Li/Li^+ to obtain cycle durability, and no attempts to extend the potential range of the activated-carbon positive electrode to a higher potential region have been reported.

On the other hand, a high-energy-density EDLC using non-porous graphitizable carbon heat-treated with potassium hydroxide (KOH-activated soft carbon) has been developed [20–23]. Mogami [22,23] Takeuchi et al. [20,21] reported that the EDLC using KOH-activated soft carbon has quite a low electrostatic capacitance due to its small specific surface area in the initial state. However, its capacitance increases significantly by the first charging process, and the capacitance exceeds that of a conventional EDLC using activated carbon. Therefore, the KOH-activated soft carbon is promising for the positive electrode of the HEC. However, as far as we know, no attempt to use this carbon for the HEC has been reported.

Therefore, this work focuses on the usage of KOH-activated soft carbon for the positive electrode in the HEC and the investigation of a suitable electrolyte. High performance of the advanced HEC using KOH-activated soft carbon as a positive electrode and non-graphitizable carbon as a negative electrode is demonstrated.

2. Experimental

2.1. Preparation of the KOH-activated soft carbon

KOH-activated soft carbon was prepared from liquid crystalline aromatic resin (AR resin, Mitsubishi Gas Chemical). The resin was ground with a mortar, and calcined at 800 °C for 2 h in an N_2 atmosphere to prepare the graphitizable carbon (soft carbon). The resulting soft carbon was mixed with small tablets of KOH (four-fold weight) in an alumina melting pot. Then, the soft carbon containing KOH was heated at 800 °C for 2 h in N_2. After cooling down, the alkali-rich residual carbon was washed with hot water until the outlet water reached pH 7. The resulting KOH-activated soft carbon was dried by heating in a vacuum.

2.2. Preparation of positive electrode

Commercially available activated carbon (steam activated, average particle size 2.9 μm, 1500 $m^2\,g^{-1}$) and KOH-activated soft carbon (average particle size 11.6 μm, 46 $m^2\,g^{-1}$) prepared by the above-mentioned method were used as the material for the positive electrode. These carbon materials were mixed with poly(tetrafluoroethylene) (PTFE) (D-210C, Daikin) and carbon black (Ketjenblack ECP, Lion Co., Ltd.) at a mass ratio of 85:10:5, stiffened by mixing in mortar, and then pressed with a roller press to control the thickness. The thickness of the carbon sheet was 100 μm in single-electrode tests, whereas the thickness of the positive electrode in full-cell tests was adjusted so that its capacity was balanced with that of the negative electrode. The resulting electrode sheet was punched out in 10-mm diameter pieces that were dried at 120 °C for 12 h and then applied by pressure to a stainless steel mesh for use as positive electrodes.

2.3. Preparation of negative electrode

Commercially available non-graphitizable carbon (average particle size 9.3 μm, 2.9 $m^2\,g^{-1}$) was used as the material for

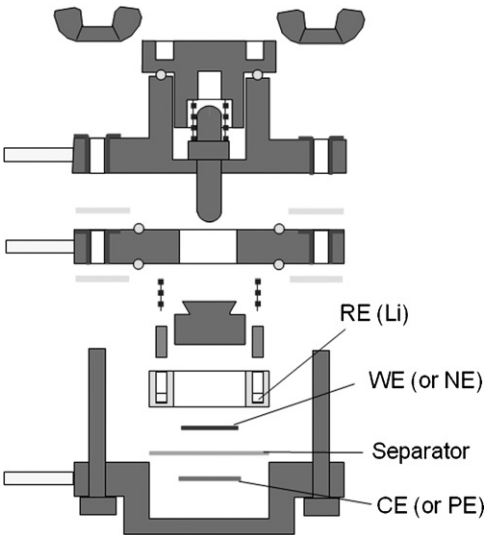

Fig. 2. Schematic of three-electrode cell made of stainless steel.

the negative electrode. Non-graphitizable carbon was mixed with poly(vinylidene fluoride) (PVdF) dissolved in *N*-methyl-2-pyrrolidone (NMP), applied to a copper foil, and heated at 80 °C for 12 min. The resulting sheet was pressed with a roller press, punched out in 10-mm diameter pieces, and then dried at 120 °C for 12 h for use as negative electrodes.

2.4. Analyses of carbon materials

Field-emission scanning electron microscopy (FE-SEM) (JSM-6320F, JOEL) was used to observe the surface of the carbon materials. The pore size distribution and crystal structure of the carbon materials were analyzed by N_2-gas adsorption apparatus (BELSORP36, BEL Japan) and X-ray diffraction (XRD) (UltraX 18 V B2, Rigaku), respectively.

2.5. Test cell fabrication and charge–discharge cycling tests

All electrochemical measurements except for the cycling test were performed with a stainless-steel three-electrode cell (Toyo System) shown in Fig. 2. The coin-type cell (CR2032) was used only in the cycling test. The electrolyte was a 1 mol dm^{-3} (1 M) solution of various lithium salts in different solvents. Lithium hexafluorophosphate ($LiPF_6$) (Kishida Chemical), lithium tetrafluoroborate ($LiBF_4$) (Kishida Chemical), lithium perchlorate ($LiClO_4$) (Kishida Chemical), lithium trifluoromethanesulfonate ($LiCF_3SO_3$) (Aldrich), lithium bis(trifluoromethanesulfonyl)imide [$Li(CF_3SO_2)_2N$] (Aldrich), lithium bis(oxalato)borate (LiBOB) (Tomiyama Chemical), and lithium tris(trifluoromethanesulfonyl)methide [$Li(CF_3SO_2)_3C$] (Covalent) were used as electrolytes. Ethylene carbonate (EC), propylene carbonate (PC), butylene carbonate (BC), dimethyl carbonate (DMC), ethylmethyl carbonate (EMC), diethyl carbonate (DEC) and γ-butyrolactone (GBL) (Kishida Chemical) were used as solvents. A glass-fiber filter (GB-100R, Advantec) and PVdF porous film (Tomoegawa) were used as separators for the stainless-steel test cell and coin-type cell, respectively. Charge–discharge cycling tests were performed with a battery tester (TOSCAT-3100, Toyo System) in a glove box filled with dry argon gas, with the results presented in terms of specific values per volume of electrode sheet, excluding the current collectors.

3. Results and discussion

3.1. Characteristics of the carbon materials

FE-SEM images and pore size distribution of the carbon materials used as active material in this study are shown in Figs. 3 and 4, respectively. There is no notable difference in these particular shapes between KOH-activated soft carbon and the others (Fig. 3). However, KOH-activated soft carbon has a much smaller number of pores, similar to non-graphitizable carbon (Fig. 4). The XRD patterns of the carbon materials are shown in Fig. 5, together with those of the soft carbon (without activation). The crystal structure of the KOH-activated soft carbon is more oriented than that of the activated carbon or non-graphitizable carbon, and the lattice distance of the 0 0 2 plane (d_{002}) for KOH-activated soft carbon is slightly larger than that before activation. Next, the electrochemical characteristics of the carbon materials were investigated using the EDLC full-cell. The charge–discharge profile of the EDLC full-cell using KOH-activated soft carbon as positive and negative electrodes is shown in Fig. 6, together with that of the EDLC using conventional activated carbon as both electrodes. It is clear that the specific capacitance of the EDLC using KOH-activated soft carbon increases significantly by the first charging, which is consistent with the results in published reports [20,21]. In this paper, the capacitance increasing behavior is referred to as "Electrochemical activation".

3.2. Optimization of the electrolyte composition

Mogami [22,23] Takeuchi et al. [20,21] suggested the mechanism for the capacitance increasing behavior that observed in an EDLC using KOH-activated soft carbon from XRD and solid-state nuclear magnetic resonance (SSNMR) results. A schematic diagram for the electrochemical activation speculated from published reports is shown in Fig. 7. The KOH-activated soft carbon has a quite low capacitance in the initial state because of its small surface area. However, ions and the solvents of the electrolyte solutions are considered to be co-intercalated into the carbon, and the capacitance increases significantly at the first charge. Therefore, the type of ion species and solvent has a crucial effect on the performance of the EDLC. Mogami [22,23] Takeuchi et al. [20,21] also reported that EMI^+, BF_4^- and acetonitrile can bring higher capacity in EDLCs, however, these reports are only on EDLCs composed of the KOH-activated soft carbon as polarizable positive and negative electrodes. EMI^+ or AN in particular are difficult to use for the HEC with lithium insertion-type carbon negative electrodes because of the cathodic decomposition. Therefore, we examined a suitable electrolyte for the HEC in this study.

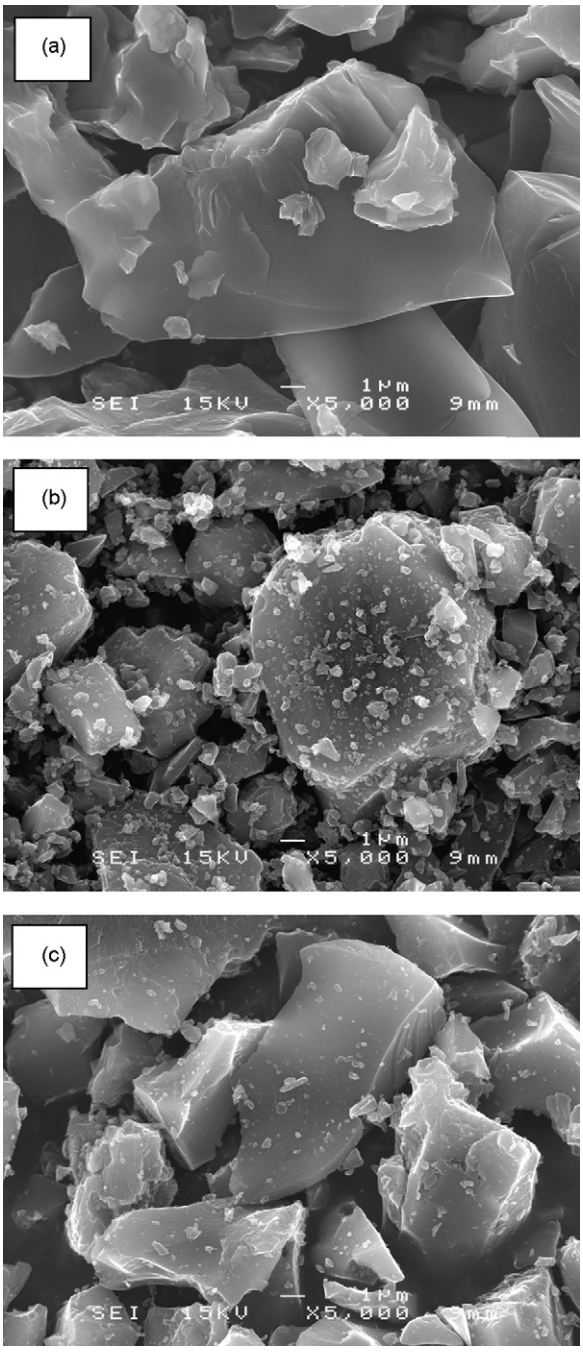

Fig. 3. FE-SEM images of carbon materials: (a) KOH-activated soft carbon, (b) activated carbon and (c) non-graphitizable carbon.

3.2.1. *Effects of the anion*

In the HEC using Li^+ insertion into negative electrode, the type of cation is not changeable. Therefore, a suitable anion for HEC is examined first. The effects of anion upon the performance are investigated through single-electrode tests using the KOH-activated soft carbon as the working electrode (WE) and Li metal as a counter electrode (CE) and a reference electrode (RE). To investigate the effect of the loading potential on the resulting capacitance, single-electrode charge–discharge tests were carried out under the conditions that the lower potential limit was 3 V (versus Li/Li^+) and the upper potential limit was

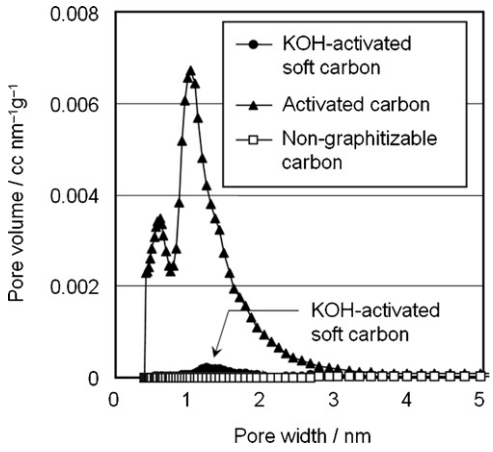

Fig. 4. Pore size distribution of (●) KOH-activated soft carbon, (▲) activated carbon and (□) non-graphitizable carbon.

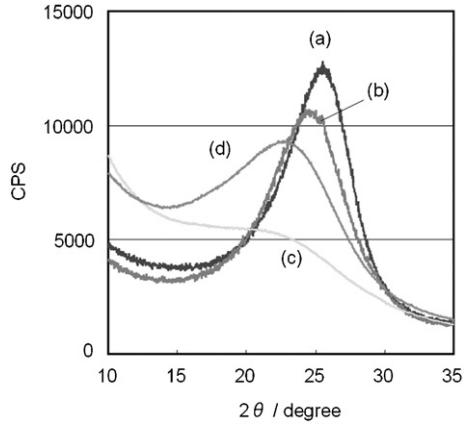

Fig. 5. XRD patterns of carbon materials: (a) soft carbon (before activation), (b) KOH-activated soft carbon, (c) activated carbon and (d) non-graphitizable carbon.

gradually changed from 3.5 to 5.5 V. Each charge–discharge cycle was given 6 times in each upper potential limit. At each 1st cycle, constant current (5 mA cm^{-2})–constant voltage (current reduced to 0.5 mA cm^{-2}) (CC–CV) charging and constant current (1 mA cm^{-2}) (CC) discharging was carried out. After

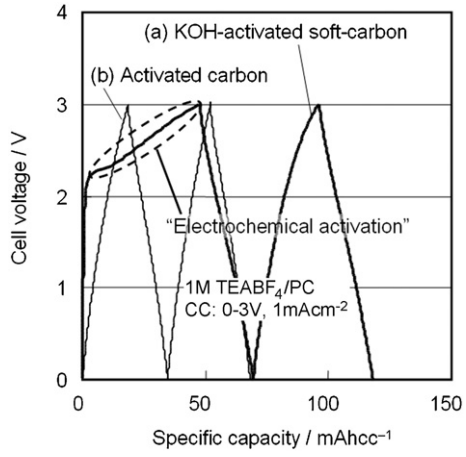

Fig. 6. Charge–discharge profiles of EDLC full-cell using: (a) KOH-activated soft carbon and (b) conventional activated carbon.

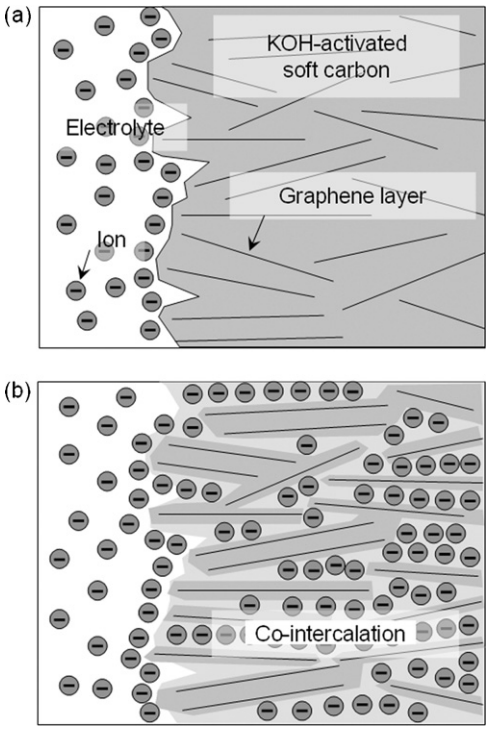

Fig. 7. Schematic diagram of electrochemical activation speculated from published reports. (a) Before first charging and (b) after first charging.

that constant current (5 mA cm^{-2}) charge and discharge cycles were carried out for following 5 cycles. The cycling test was terminated if the constant voltage charging continued over 10 h. The specific capacitance of each upper potential limit was calculated from each 6th discharge profile using the following equation:

$$SC = 2(U - 3It)(E - 3 - \Delta E)^{-2}\ V^{-1} \quad (1)$$

where SC is the specific capacitance per volume, U the discharging energy based on the potential at 0 V (versus Li/Li^+), I the discharge current, t the discharge time length, E the charging cut off voltage based on the potential at 0 V, ΔE the IR-drop loss voltage and V is the volume of the electrode sheet excluding the current collector. Each parameter is schematically explained in Fig. 8. The resulting specific capacitance and the internal resistance are shown in Fig. 9 as a function of the loading potential. In almost all anions, the specific capacitance increases significantly with a loading potential over 4 V. The specific capacitance decreases and the internal resistance increases when the potential exceeds a certain value. The capacitance decrease indicates the anodic decomposition of the anion and/or solvent. From these results, it was found that PF_6^- is the best anion because the electrolyte gives higher capacitance, higher voltage stability and lower internal resistance. Although the anion ClO_4^- gave also high specific capacitance, its anodic stability was slightly lower than PF_6^-. The BF_4^- anion was expected to give high specific capacitance and high potential stability, as respond for EDLC using KOH-activated soft carbon [20–23], and higher potential stability than ClO_4^- in linear sweep voltammetry (LSV) using a glassy carbon-working electrode [24]. In this work, however,

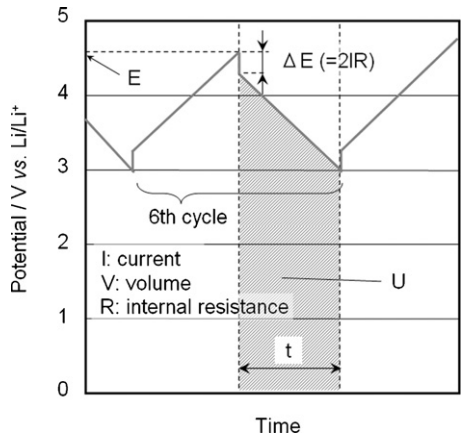

Fig. 8. Schematic explanation of several parameters used for calculation of electrostatic capacitance and internal resistance.

the electrolyte using BF_4^- decomposed at lower potential than that using ClO_4^-. These results are somewhat inconsistent with that of published reports on electrochemical stability evaluated by LSV [24]. It is considered that the mechanism at the KOH-activated soft carbon might be different from that at glassy carbon.

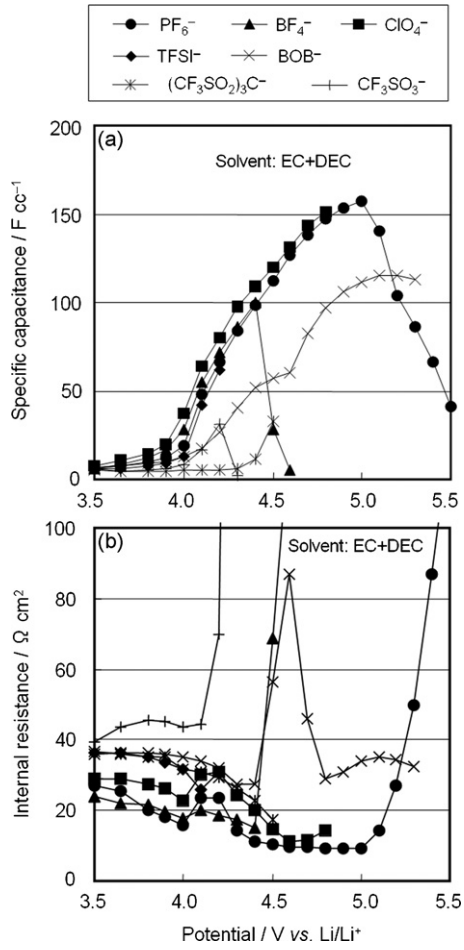

Fig. 9. Specific capacitance and internal resistance for KOH-activated soft carbon as a function of loading potential using different types of anion species.

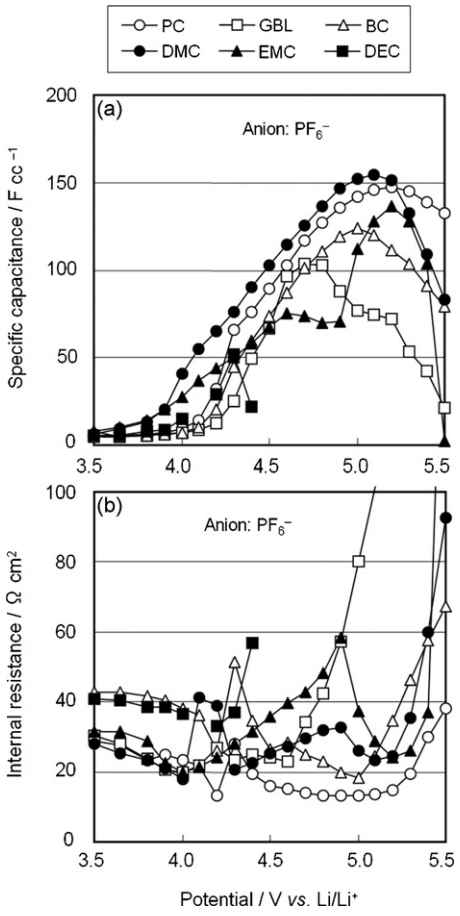

Fig. 10. Specific capacitance and internal resistance for KOH-activated soft carbon as a function of loading potential using different types of solvent.

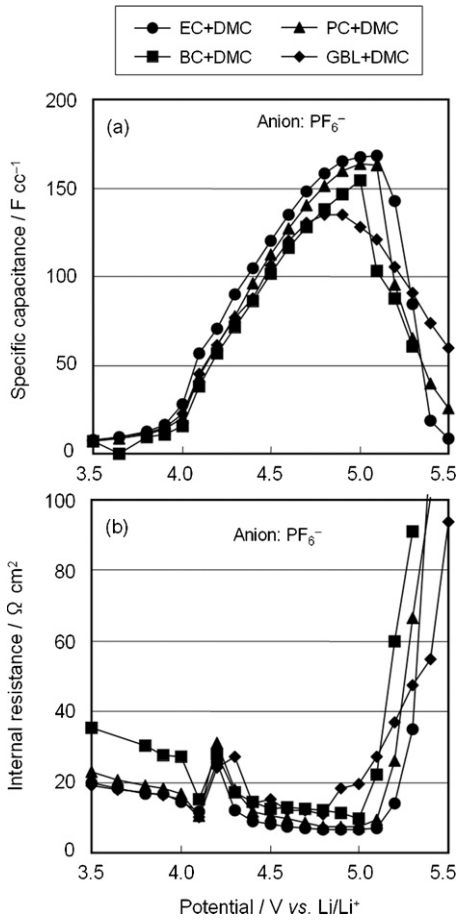

Fig. 11. Specific capacitances and internal resistances for KOH-activated soft carbon as a function of loading potential using various DMC based binary solvent.

3.2.2. *Effects of the solvents*

Next, the effects of solvents were investigated. First, single solvents dissolving $LiPF_6$ were investigated using the same method as described in the previous section. The specific capacitance and internal resistance of KOH-activated soft carbon are shown in Fig. 10 as a function of the loading potential in the different single solvent system. DMC and PC show higher capacitance and higher potential stability. The other solvents, especially DEC, have either lower capacitance and/or lower anodic stability. From these results, it was found that DMC is good solvent for obtaining high capacitance. However, DMC gives slightly higher internal resistance, and it is difficult to use DMC alone because of its low boiling point and high vapor pressure at room temperature. Therefore, DMC-based binary solvents are evaluated next.

The specific capacitance and internal resistance of KOH-activated soft carbon in various DMC-based binary solvents are shown in Fig. 11 as a function of the loading potential. From these results (together with the results of Figs. 9 and 10), the binary solvent consisting of EC and DMC gives the highest capacitance and lowest internal resistance. In total, it was found that $LiPF_6$ dissolved in EC mixed with DMC is the most suitable for the advanced HEC using KOH-activated soft carbon for positive electrode.

The specific capacitance and internal resistance of KOH-activated soft carbon and conventional activated carbon are comparatively shown in Fig. 12, where the binary solvent of EC and DMC is used for the KOH-activated soft-carbon, and the binary solvent of EC and DEC is used for conventional activated carbon. It is clear that the capacitance, the potential stability and the internal resistance of the KOH-activated soft carbon are all vastly superior to compared with those of the conventional activated carbon. Therefore, the advanced HEC using KOH-activated soft carbon for positive electrode is expected to give high energy density and high power density.

3.3. *Full-cell tests*

Next, the full-cell of the advanced HEC using KOH-activated soft carbon for positive electrode and non-graphitizable carbon for negative electrode was fabricated with the optimized electrolyte composition, and its performances are evaluated. In this cell, a punctured lithium foil was placed between positive and negative electrodes to prevent the capacity loss of the negative electrode due to deposition of byproduct at the positive electrode [25]. The charge–discharge profiles for the conventional EDLC, the conventional HEC and the advanced HEC are shown in Fig. 13. Lithium pre-doping was not carried out in both HECs.

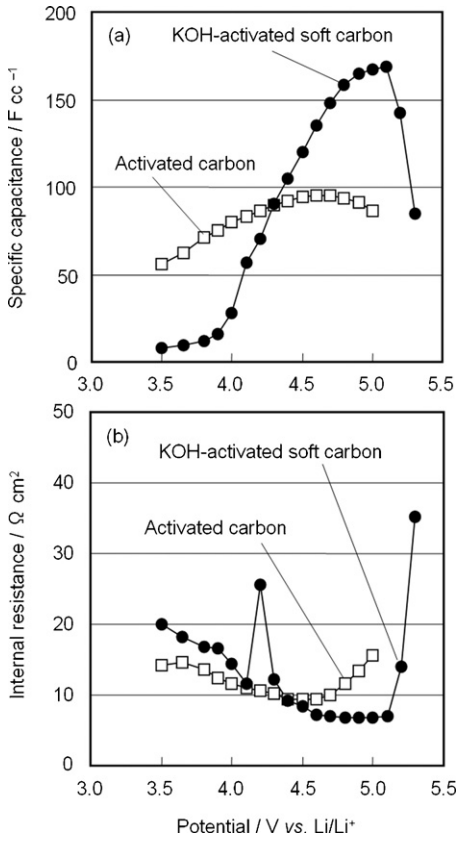

Fig. 12. Specific capacitance and internal resistance of (●) KOH-activated soft carbon and (□) conventional activated carbon as a function of the loading potential. The binary solvent mixed with EC and DMC and the binary solvent mixed with EC and DEC are used for KOH-activated soft carbon and activated carbon, respectively.

The optimum volume ratio of the positive electrode to the negative electrode for HEC was determined to equalize the capacities to both electrodes in the first charge. The capacity including irreversible capacity of the KOH-activated soft carbon (3.0–4.7 V versus Li/Li$^+$) is about 3 times higher than that of the conventional activated carbon (3.0–4.0 V versus Li/Li$^+$). Therefore, the volume ratios for the conventional HEC and advanced HEC were determined to 9:1 and 3:1, respectively. Mainly due to the reduction in the amount (volume) of the positive electrode material, the advanced HEC has significantly higher capacity than the others. All disordered carbon including the non-graphitizable carbon has certain irreversible capacity from about 15–30% in the first cycle. In the conventional HEC without Li pre-doping, the activated carbon positive electrode cannot be discharged fully due to the irreversible capacity of the carbonaceous negative electrode (ca. 29%). Whereas, in the advanced HEC, the irreversible capacity of the KOH-activated soft-carbon positive electrode (ca. 50%) compensates that of carbonaceous negative electrode, and enables the positive electrode to be discharged up to a lower potential region. This effect is equivalent to the lithium pre-doping process of the negative electrode in proposed HEC [7,8].

Next, the energy density and power density of these full-cells were calculated. Fig. 14 shows the Ragone plots obtained by the tests under CC (1 mA cm^{-2})–CV (reduced to 0.5 mA cm^{-2})

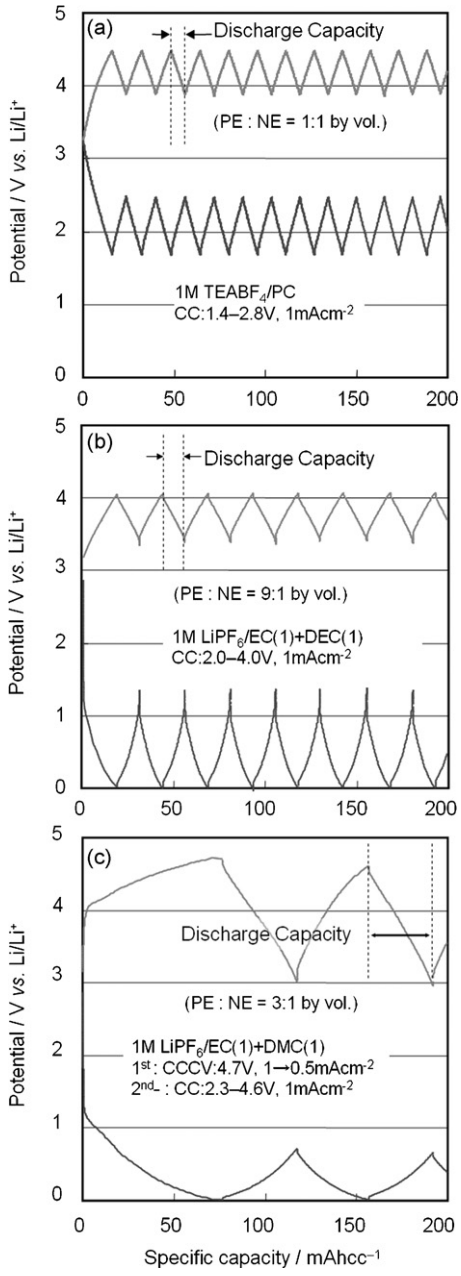

Fig. 13. Charge–discharge profiles for (a) conventional EDLC, (b) conventional HEC and (c) advanced HEC.

charging followed by constant power (CP) discharging. The energy density at low power density of discharge (under 100 W L^{-1}) and the power density that can be delivered during continuous discharge for 10 s are summarized in Table 1. The advanced HEC clearly shows higher energy density and higher power density than the others. The energy density is about 8.5 times as high as that of the EDLC, and the power density is about 4.6 times as high.

A cycling test of the advanced HEC was carried out using a coin-type cell. The capacity retention and the coulombic efficiency in the early cycle are shown in Fig. 15. No capacity loss and high coulombic efficiency were observed in these initial 300 cycles.

Table 1
Energy densities and power densities for conventional EDLC, conventional HEC, and advanced HEC

	Energy density		Power density	
	Volume [Wh L^{-1}]	Weight[a] [Wh kg^{-1}]	Volume [Wh L^{-1}]	Weight[a] [Wh kg^{-1}]
Conventional EDLC (1.4–2.8 V)	15.8	24.1	3041	4646
Conventional HEC (2.0–4.0 V)	40.2	56.4	3519	4941
Advanced HEC (2.3–4.6 V)	134.0	145.1	13936	15092

Energy densities were obtained by the tests under CC (1 mA cm^{-2})–CV (reduced to 0.5 mA cm^{-2}) charging followed by low power density of discharging (under 100 W L^{-1}). Power densities were obtained using the maximum power that can be delivered during continuous discharge for 10 s.
[a] Based on the total weight of the active materials.

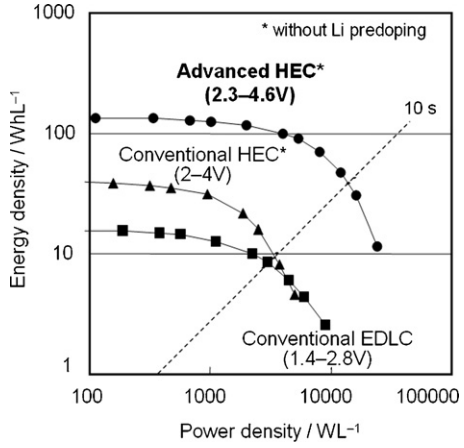

Fig. 14. Ragone plots for (■) conventional EDLC, (▲) conventional HEC and (●) advanced HEC obtained by the tests under CC (1 mA cm^{-2})–CV (down to 0.5 mA cm^{-2}) charging followed by constant power (CP) discharging.

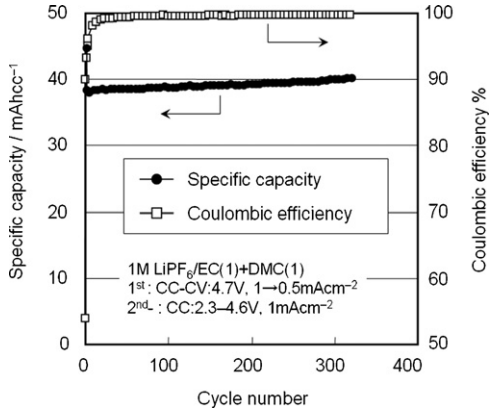

Fig. 15. Capacity retention and coulombic efficiency of the advanced HEC using KOH-activated soft carbon for positive electrode and non-graphitizable carbon for negative electrode in the early cycles.

4. Conclusions

We investigated an advanced HEC using KOH-activated soft carbon prepared from liquid crystalline aromatic resin for positive electrode and non-graphitizable carbon for negative electrode to improve the energy density of the device. The experimental results are summarized as follows:

(1) The KOH-activated soft carbon showed the best performances, such as high capacitance, good potential stability and low internal resistance, with the electrolyte solution consisting of binary solvent of EC and DMC dissolving $LiPF_6$.
(2) The full-cell of the advanced HEC, which is composed of the KOH-activated soft carbon for positive electrode and non-graphitizable carbon for negative electrode gives excellent energy and power densities due to the high capacity of the KOH-activated soft carbon and offset for the irreversible capacity of both electrode. The energy density reaches 8.5 times as high as that of the EDLC, and the power density reaches 4.6 times as high.

References

[1] M. Iwaida, N. Oki, S. Oyama, K. Murakami, M. Noguchi, Proceedings of the 13th International Seminar on Double Layer Capacitor and Hybrid Energy Storage Devices (Florida), December 8–10 (Dec. 9 Paper #5), 2003.
[2] S. Nishikawa, M. Sasaki, A. Okazaki, S. Araki, T. Miyata, M. Nishina, JSAE Rev. 24 (3) (2003) 249–254.
[3] D.Y. Jung, Y.H. Kim, S.W. Kim, S.-H. Lee, J. Power Sources 114 (2003) 366–373.
[4] G.G. Amatucci, F. Badway, A.D. Pasquier, T. Zheng, J. Electrochem. Soc. 148 (2001) A930.
[5] T. Morimoto, M. Tsushima, G. Cha, Y. Che, in: R.J. Brodd, D.H. Doughty, J.H. Kim, M. Morita, K. Naoi, G. Nagasubramanian, C. Nanjundiah (Eds.), Hybrid Capacitor and Hybrid Power Sources, PV 2002-7, The Electrochemical Society Proceedings Series, Pennington, NJ, p. 161, 2002.
[6] A. Yoshino, T. Tsubata, M. Shimoyamada, H. Satake, Y. Okano, S. Mori, S. Yata, J. Electrochem. Soc. 151 (2004) A2180.
[7] O. Hatozaki, In Proceedings of the Advanced Capacitor World Summit 2005, In-intertech Corp., 2005.
[8] T. Aida, K. Yamada, M. Morita, Electrochem. Solid-State Lett. 9 (2006) A534.
[9] A.D. Pasquier, I. Plitz, J. Gural, S. Menocal, G.G. Amatucci, J. Power Sources 113 (2003) 62.
[10] A.D. Pasquier, I. Plitz, S. Menocal, G.G. Amatucci, J. Power Sources 115 (2003) 171.
[11] T. Brousse, R. Marchand, P. Taberna, P. Simon, J. Power Sources 158 (2006) 571.
[12] Y. Wang, J. Luo, C. Wang, Y. Xia, J. Electrochem. Soc. 153 (2006) A1425.
[13] T.Y. Chang, X. Wang, D.A. Evans, S.L. Robinson, J.P. Zheng, J. Power Sources 110 (2002) 138.
[14] J.H. Park, O.O. Park, J. Power Sources 111 (2002) 185.
[15] T. Brousse, M. Toupin, D. Bélanger, J. Electrochem. Soc. 151 (2004) A614.
[16] Y. Wang, L. Yu, Y. Xia, J. Electrochem. Soc. 153 (2006) A743.
[17] V. Khomenko, E. Raymundo-Piñero, F. Béguin, J. Power Sources 153 (2006) 183.
[18] E. Frackowiak, V. Khomenko, K. Jurewicz, K. Lota, F. Béguin, J. Power Sources 153 (2006) 413.

[19] S. Nohara, T. Asahina, H. Wada, N. Furukawa, H. Inoue, N. Sugoh, H. Iwasaki, C. Iwakura, J. Power Sources 157 (2006) 605.
[20] M. Takeuchi, K. Koike, T. Maruyama, A. Mogami, M. Okamura, Electrochemistry 66 (1998) 1311.
[21] M. Takeuchi, T. Maruyama, K. Koike, A. Mogami, T. Oyama, H. Kobayashi, Electrochemistry 69 (2001) 487.
[22] A. Mogami, OyoButsuri 73 (2004) 1076.
[23] A. Mogami, Nikkei Electron. 6 (2004) 131.
[24] M. Ue, M. Takeda, M. Takehara, S. Mori, J. Electrochem. Soc. 144 (1997) 2684.
[25] T. Aida, I. Murayama, K. Yamada, M. Morita, Electrochem. Solid-State Lett. 10 (2007) A93.